

Theoretical investigation of optical absorption process and J-V characteristics in nanostructured CuPc-C60 bilayer solar cells

Y. AZIZIAN-KALANDARAGH^{a,b*}, M. DOURNAMA^c, A. ABDOLAHZADEH-ZIABARI^d

^aDepartment of Physics, Mohaghegh Ardabili University, Ardabil, Iran

^bDepartment of Engineering Sciences, Sabalan University of Advanced Technologies, Namin, Iran

^cPayam Nour University of Urmia, Urmia, Iran

^dNano Research Lab, Lahijan Branch, Islamic Azad University, P.O. Box: 1616, Lahijan, Iran

In this research, optical absorption processes have been studied for a specific type of nanostructured organic solar cells with a donor-acceptor polymer-fullerene active layer using the Fresnel absorption and transfer coefficients by optical transfer matrix model. Two different structures, $SiO_2 - ITO - PEDOT:PSS - CuPC - C_{60} - Al$ and $SiO_2 - ITO - CuPC - C_{60} - Al$ have been proposed for this simulation. Initially, we explored the wavelength-dependent optical absorption in the case of the proposed devices, and the analyses, showed a maximum optical absorption in a wavelength of about 600nm. Then, we determined the normalized modulus square electric field (E^2) and energy dissipation factor (Q) for different thicknesses of active layer in a given wavelength (600nm). Also, we obtained the optimum thicknesses in the case of all layers in 600nm incident wavelength. In the next step, we determined power conversion efficiency for two proposed structures. The results showed that, the presence of a thin layer of PEDOT: PSS reveals an increase in the efficiency of the device. By providing the possibility of controlling the thickness-dependent optical properties, these types of simulations could help technologists to design and propose solar cell devices with high efficiencies.

(Received March 13, 2015; accepted June 9, 2016)

Keywords: Organic solar cells, Theoretical modeling, Optical absorption, Semiconductor, Power conversion efficiency

1. Introduction

The production of cost effective, green and renewable energy sources have attracted many scientists and engineers in recent years because of their useful applications and interesting theoretical natures. In last several years, theoretical and experimental investigations of solar cells have caught many attentions due to the important necessity of solar cells to produce solar energy as a suitable renewable energy source [1-7].

Organic-semiconductor solar cells are based on the concept of electron and hole separation at an interface of two contacts are also attracting a great deal of attention because of easier electrical and optical parameters tunability, low cost, flexibility, and large- area applications [8-12]. From experimental point of view, the fabrication of device, have some technological difficulties in the first step, it is necessary to use pure and suitable materials to prepare multilayer structures. The consideration of some factors such as type of organic and inorganic materials, type of junctions, purity of materials, thicknesses, doping materials, morphology and structure of the layer and interfaces their suitable and stable optical and electrical properties for sun light, etc are necessary and important [13].

Recently, an important progress has been made on the improvement of the stability and power conversion efficiencies of organic-semiconductor solar cell devices

and the achieved efficiencies have been reported by many researchers [14-16].

To date, this field has been dominated by solid-state junction devices, usually made of silicon, and profiting from the experience and material availability resulting from the semiconductor industry. The dominance of the photovoltaic field by inorganic solid-state junction devices is now being challenged by the emergence of a third generation of cells, based, e.g. on nanocrystalline oxide and conducting polymers films. These offer the prospective of very low-cost fabrication and present attractive features that facilitate market entry. It is now possible to depart completely from the classical solid-state cells which are replaced by devices based on interpenetrating network junctions. Nanophase structure of the polymer layer has a huge impact on the characteristics of the device and its performance. Various architectures of the polymer solar cells and effect of the morphology on the characteristics of solar cells have been investigated. In this study different structures of organic bilayer with layers of donor - acceptor have been studied.

In these structures polymers of CuPC(Copper PthaloCyalline) and C60(fullerene) have the role of the donor and acceptor, respectively. Light is absorbed by the donor layer and the production and diffusion of the exciton occurs in that layer and excitons are reaching the p-n interface, and transport and collection of the charge occurs at the electrodes. In this study, exciton diffusion length

(10-20nm) is intended and is obtained maximum efficiency in maximum diffusion length. Absorption of sunlight by a single layer depends on the layer thickness and optical constants. Also with placing PEDOT: PSS layer between the anode and absorbent layer improves the performance of solar cells [17-19].

In this paper, regarding to achieve high power efficiency in the case of two proposed structures, ($SiO_2 - ITO - PEDOT: PSS - CuPC - C_{60} - Al$ and $SiO_2 - ITO - CuPC - C_{60} - Al$) we obtained and optimized some optical parameters. These parameters are primary factors which are necessary in understanding the solar cell devices mechanisms.

2. Theory and simulation

2.1. Transfer matrix method

In this research, transfer matrix method has been used for investigation of optical processes and simulation of the optical field distribution which occurs in multilayer optical devices. This method has been developed by many researchers [20-23].

Normalized modulus of the electromagnetic field at an arbitrary location within the layer is:

$$E_j(z) = E_0^+ \frac{M'_{j,11} e^{i\xi j(z-dj)} + M'_{j,21} e^{i\xi j(dj-z)}}{M'_{j,11} M'_{j,11} e^{i\xi j(dj)} + M'_{j,12} M'_{j,21} e^{i\xi j(dj)}} \quad (1)$$

where, E_0^+ is the electric field of the incident wave. Energy dissipation parameter (Q) in the depth z in the material (that is a measure of absorption) for the wavelength λ in terms of $W \cdot m^{-2} \cdot nm^{-1}$ is obtained as:

$$Q(z) = \frac{1}{2} c \varepsilon_0 \alpha n |E(z)|^2 \quad (2)$$

where ε_0 is the permittivity of free space, n is the refractive index, c is the speed of light, and α stands for the absorption coefficient.

2.2. Simulation of energy conversion processes

For determining the limits of the power conversion efficiency of organic solar cells, we use a model on the base of optical models which is presented in reference [18].

Light beam is radiated to donor layer and is absorbed in absorbent layer. After absorbing light, electron is excited from the donor highest occupied molecular orbital (HOMO) level to its lowest unoccupied molecular orbital (LUMO) (so-called exciton generation process). Then exciton in distance of diffusion length in this layer is diffused and reaches the p-n interface. At this moment electrons will move from the acceptor LUMO level to the donor LUMO level and holes in the opposite direction. This charge transport process is named separation of exciton. In the next step, electron will move from the

acceptor LUMO level to the cathode and holes from the donor HOMO level to the anode, thus current is created.

Internal quantum efficiency is product of four efficiencies, corresponding to four steps in the charge generation process:

$$\eta_{IQE} = \eta_A \times \eta_{ED} \times \eta_{CT} \times \eta_{CC} \quad (3)$$

$$\eta_A = (1 - e^{-\alpha d}) \quad (4)$$

where η_A denotes the absorption efficiency within the active region of the solar cell, d stands for active layer thickness, and α is the absorption coefficient. The coefficient η_{ED} called the exciton diffusion efficiency to the region of separation is given as:

$$\eta_{ED} = e^{-d/L_d} \quad (5)$$

where L_d is the exciton diffusion length.

Meanwhile, the coefficient η_{CT} in Eq.3 is the charge transport efficiency, which is the efficiency for separation of an exciton into a free electron and hole pair at the site. Also, η_{CC} is the charge collection efficiency in the equation.

In general, it has been found that the charge collection and charge transfer efficiencies at organic donor/acceptor interfaces commonly used in thin-film molecular organic semiconductor PV cells approach 100%, in which the internal quantum efficiency is determined by the product of $\eta_A \times \eta_{ED}$. The internal quantum efficiency of bilayer solar cells is restricted by exciton diffusion to p-n interface or photon absorption processes [18]. If the thickness of p-n films were thicker than L_D , due to increased η_A and reduced η_{ED} , the number of generated excitons reaching the p-n interface would be dropped drastically. Thus, it has to be a balance between η_A and η_{ED} . The highest internal quantum efficiency will be obtained when the thickness of the donor and acceptor is balanced in a way that $\eta_A \times \eta_{ED}$ gives the maximum amount [17].

For bilayer heterojunction solar cells, exciton diffusion length is about 0-20 nm.

Internal quantum efficiency ($\eta_A \times \eta_{ED}$) versus $\frac{d}{L_d}$ for diffusion lengths of 10, 15, and 20 nm and thickness of absorbent layer in the range of 1-100 nm have been drawn for both structures. For each structure, diagram shows a peak in $\frac{d}{L_d}$ that this point is not practical, because the layer thickness is greater than the diffusion length. Assuming the maximum exciton diffusion length of 20 nm and optimum thickness that determined previously, the internal quantum efficiency is obtained for that point.

The external quantum efficiency (the ratio of total number of electrons produced to the photons that come to the structure) is related to the internal quantum efficiency by the following equation:

$$\eta_{EQE} = (1 - R) \times \eta_{IQE} = (1 - R) \times \eta_A \times \eta_{ED} \times \eta_{CT} \times \eta_{CC} \quad (6)$$

where R is the reflection of glass–air interface. With plotting diagram of the external quantum efficiency versus optimal thickness, percent of η_{EQE} is obtained. This value is important, because can give the photocurrent value according to the following equation:

$$\eta_{EQE} = \frac{h.c.j_{sc}}{\lambda.e.p_0} \quad (7)$$

where j_{sc} is the short circuit current density, p_0 is the power of incident light, e is the electron charge, h is the Planck constant and c is the speed of light in vacuum[16].

With plotting j_{sc} versus thickness of absorber layer its value can be obtained in optimal thickness.

Then, the power conversion efficiency (ratio of output power to the power of optical radiation) can be achieved from j-v diagram. Open circuit voltage and current in an actual p-n connection is calculated from the following equation:

$$V_{oc} = \frac{nkT}{q} \ln\left(\frac{j_{sc}}{j_0} + 1\right) \quad (8)$$

$$j = j_0 \left(\frac{qv}{e^{nkT}} - 1 \right) - j_{sc} \quad (9)$$

here j_0 denotes the saturation current density .

With plotting j-v diagram for diode under dark and light, the maximum values for I and V and also fill factor are achieved.

$$FF = \frac{V_m I_m}{V_{oc} I_{sc}} \quad (10)$$

The power conversion efficiency is defined as:

$$PCE = \frac{V_{oc} j_{sc} FF}{P_{in}} \quad (11)$$

and is gained for the present structures from j-v diagrams. These parameters under standard conditions (air mass AM1.5, the radiant power density 1000 W/m^2 and temperature of 25°C) are defined. To improve the device efficiency, FF factor j_{sc} and V_{oc} should be maximum [13].

3. Results and discussion

Two proposed structures that were investigated above have the following arrangements:

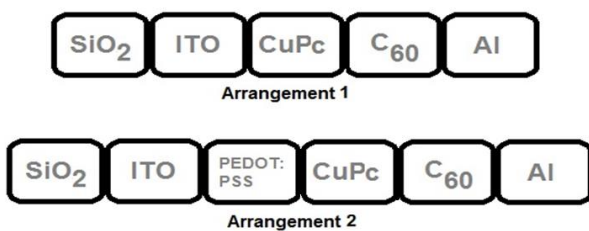


Fig. 1. The structure of two arrangement of nanostructured CuPc:C60 bilayer solar cells

In these structures, at first, the light is irradiated on the surface of SiO₂ film. It is clear that the optical behavior of the light in such multilayer system, depends on the optical parameters of the constitutive layers like refractive index and extinction coefficient. In the first stage, using transfer matrix method, the spectrum of absorption coefficient versus wavelength in the case of active layer (CuPc) is plotted for both structures. The results of the analyses show the maximum absorption coefficient at the wavelengths of 600nm. The spectra for absorption and reflection versus wavelength are plotted for the entire device in $\lambda=600\text{nm}$. In the next stage, the absorption and reflection spectra are plotted for all layers (entire device) and using these results, the amount of absorption percent is calculated.

It is known that the absorption and reflection parameters of materials are given by Fresnel relationships:

$$A=1-R \quad (12)$$

Here R is the reflection and A is the absorption. Also, in this calculation, the optimum thicknesses of layers have been calculated using the abovementioned theory for constant wavelength, refractive index and extinction coefficient. Absorption efficiency diagram versus wavelength for absorber layer reveals the maximum absorption efficiency in the same wavelength.

Considering the optimum thickness and changing the thickness, the normalized modulus squared of the optical electric field and energy dissipation is plotted. Q is not continuous in interfaces, because the excitation coefficient changes in the interfaces strongly.

Diagrams show that this thickness is optimal (for active layer) [9, 16-18].

3.1. Investigation of optical absorption process for proposed arrangement 1 (SiO₂/ITO/CuPc/C60/Al)

Fig. 2 shows the absorption coefficient of absorber layer in visible spectrum of sunlight ($\lambda=400\text{-}700\text{nm}$). Some parameters like refractive index and extinction coefficient of the materials derive from literature [19] in this calculation.

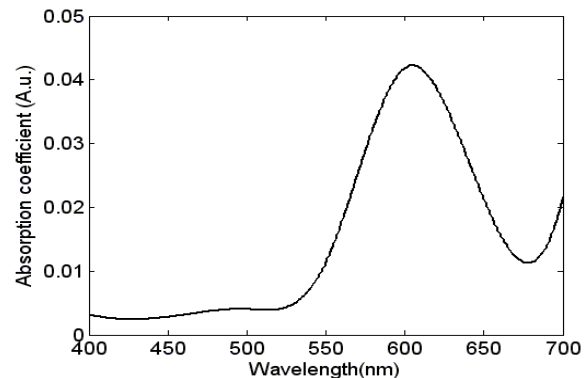


Fig. 2. Absorption coefficient versus wavelength for CuPc

As it comes from the figure, the absorption in this layer is maximum in $\lambda = 600\text{nm}$. In this wavelength, absorption and reflection for entire device are plotted for the following thicknesses:

$$d_{\text{SiO}_2} = 1\text{mm}/d_{\text{ITO}} = 100\text{nm}/d_{\text{CuPC}} = 50\text{nm}/d_{\text{C}_{60}} = 30\text{nm}/d_{\text{Al}} = 100\text{nm}$$

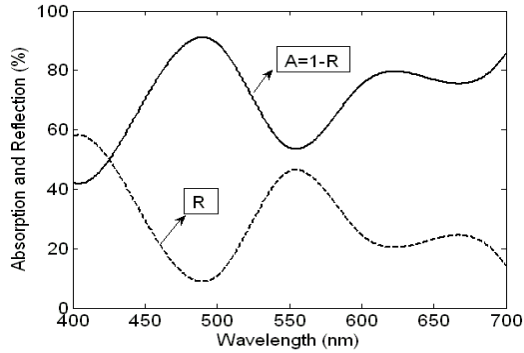


Fig. 3. Absorption and reflection for the entire device in $\lambda=400\text{-}700\text{nm}$

In $\lambda = 600\text{nm}$, 80% of incident light is absorbed in entire layers and 20% is reflected. In $\lambda = 480\text{nm}$, absorption is maximum but this wavelength is not appropriate because absorption in absorber layer is less than other wavelengths when the absorption value in absorber layer is more important due to occurrence of light absorption and exciton generation within it as is confirmed by Fig. 4.

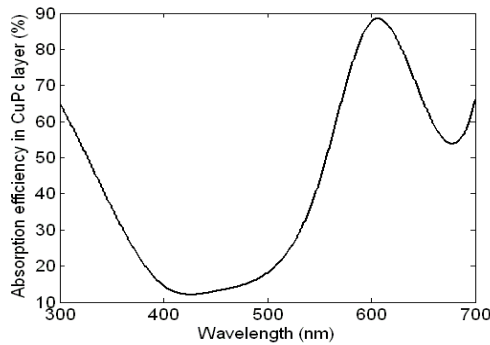


Fig. 4. Absorption efficiency versus wavelength in CuPc layer

Fig. 4 shows the absorption efficiency in CuPC layer in $d=50\text{nm}$. In $\lambda = 600\text{nm}$, the absorption efficiency in CuPc layer is maximum. This efficiency is almost 89%. It means, 89% of the absorbed light in device is absorbed by CuPc layer.

Fig. 5 show $|E|^2$ variation in device for $\lambda = 600\text{nm}$ and $d=50\text{nm}$ and 80nm where the thickness of 50nm is optimal. The change of $|E|^2$ versus distance from SiO_2/ITO interface is plotted at $d=50\text{nm}$. Furthermore, it can be easily seen that $|E|^2$ is continuous in interface of layers.

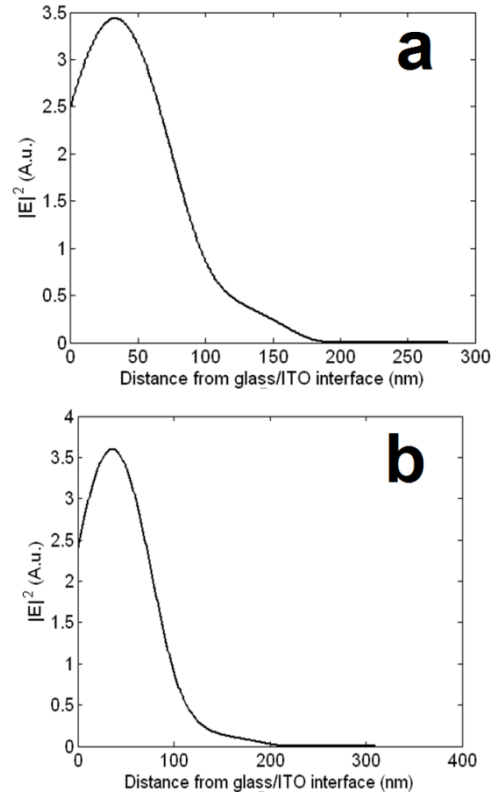


Fig. 5. $|E|^2$ Versus distance from SiO_2/ITO interface, (a): $d=50\text{nm}$; (b): $d=80\text{nm}$

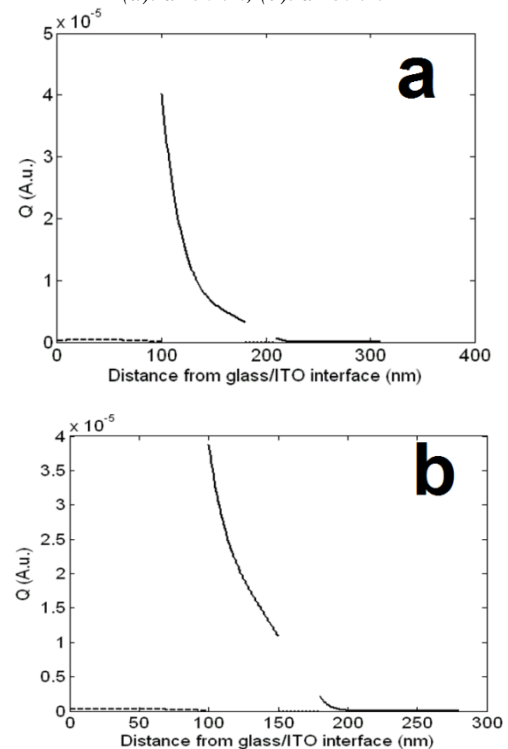


Fig. 6. Q Versus distance from SiO_2/ITO interface, (a): $d=50\text{nm}$; (b): $d=80\text{nm}$

From Figs. 6 (a) and (b), where Q is shown against thickness of layers, the absorption in ITO layer is minimum while it is maximum for absorber layer as a part of active layer.

On the other hand, the value of Q is higher for CuPc layer in $d=50\text{nm}$. Along with the plots showing changes in $|E|^2$, Q variations also affirm that in $d=50\text{nm}$, the absorption in active layer is maximum that seems optimum and desirable for our structure. Internal quantum efficiency can now be drawn for the structure 1 in diffusion lengths of 10, 15, and 20nm.

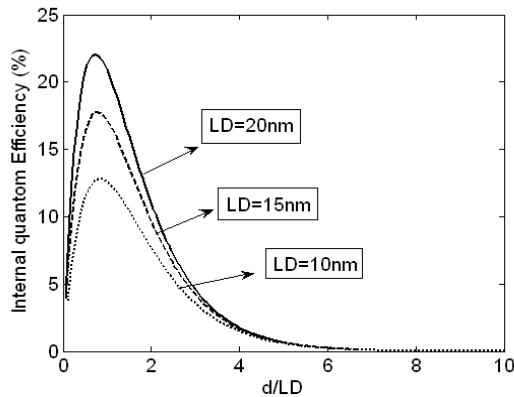


Fig. 7. Internal quantum efficiency versus d/L_D in various diffusion lengths

From the figure, the efficiency peak increases with increasing exciton diffusion length. In diffusion length of $L_D=20\text{nm}$ and $d=50\text{nm}$ for CuPc layer, $d/L_D=2.5$ and $\eta_{IQE}=7\%$.

Efficiency peak in different values of d/L_D is 75% that is not practical because layer thickness always is higher than diffusion length. Maximum efficiency can be occurred in $d \sim L_D$ and $d < 20\text{nm}$ owing to very low values of photocurrent and power conversion efficiency. Besides, for $d=50\text{nm}$, $\eta_{EQE}=5.42\%$ is obtained. The purpose of calculating η_{EQE} is to obtain the value of J_{sc} (Short-circuit current density)

In $\lambda=600\text{nm}$ and with consider to η_{EQE} , according to formula 10, in optimal thickness, $j_{sc}=1.16\text{ mA/cm}^2$ is achieved.

With plotting $j-v$ diagram, the power conversion efficiency might be evaluated.

Fig. 8 shows j_{sc} versus voltage under dark and light conditions. The point P_m shown in the figure under light condition implies the maximum power because the product of $j.v$ in this point is maximum. In this point $J_m=1\text{ mA/cm}^2$, $V_m=0.16\text{V}$; at $V=0$, $J=J_{sc}=1.16\text{ mA/cm}^2$; at $j=0$, $V=V_{oc}=0.21\text{V}$ (open circuit voltage). Plus, Fill factor can be achieved from the diagram and equals to 0.66. Hence, we do have $PCE=2.24\%$.

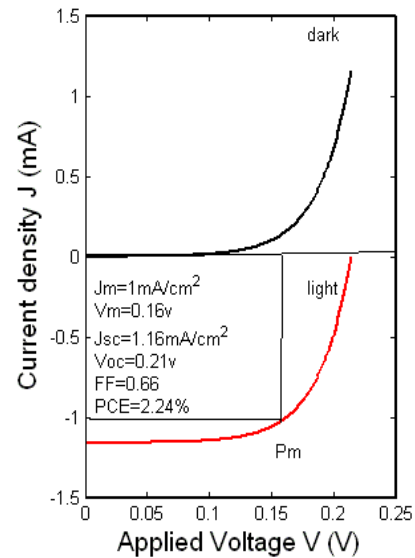


Fig. 8. Current density versus applied voltage under dark and light for Arrangement 1

3.2. Investigation of optical absorption process for proposed arrangement 2 (SiO₂/ITO/PEDOT:PSS/CuPc/C60/Al)

This structure is as the same of the previous structure just adding a surplus PEDOT:PSS thin layer between ITO and CuPc.

PEDOT:PSS {Poly (3,4-ethylenedioxythiophene) poly(styrenesulfonate)} is a material that increases the internal electric field and so the performance of the solar cell.

Fig. 9 shows the absorption efficiency of absorber layer considering the following thicknesses:

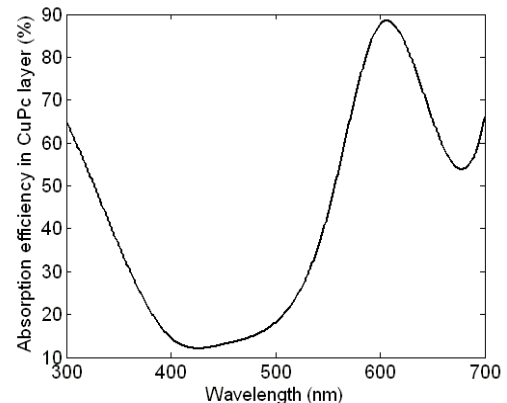


Fig. 9. Absorption efficiency versus sunlight wavelength for arrangement 2

$$d_{\text{SiO}_2} = 1\text{nm} / d_{\text{ITO}} = 110\text{nm} / d_{\text{PEDOT}} = 100\text{nm} / d_{\text{CuPc}} = 50\text{nm} / d_{\text{C}_{60}} = 30\text{nm} / d_{\text{Al}} = 100\text{nm}$$

Absorption efficiency in $\lambda=600\text{nm}$ reaches the maximum value of 90%. Besides, absorption in the entire device at this wavelength is 83%. In this wavelength Q and E^2 diagrams are plotted for $d(\text{CuPc})=50\text{nm}$ and 60nm .

Similar to the arrangement 1, an efficient and sharp absorption can be seen at this wavelength for $d=50\text{nm}$.

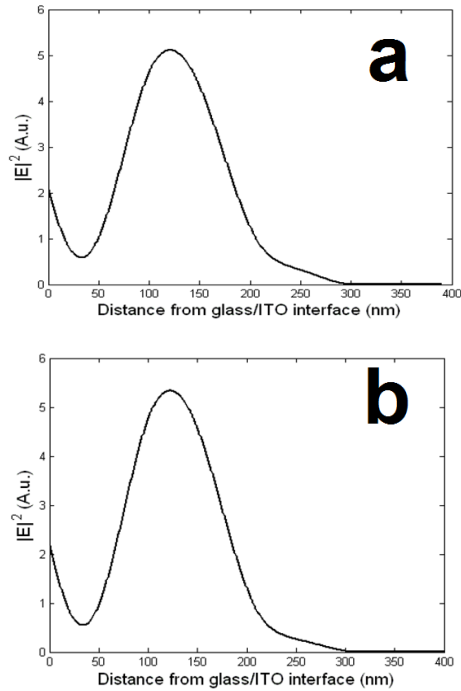


Fig. 10. $|E|^2$ versus distance from SiO_2/ITO interface, (a): $d=50\text{nm}$; (b): 60nm

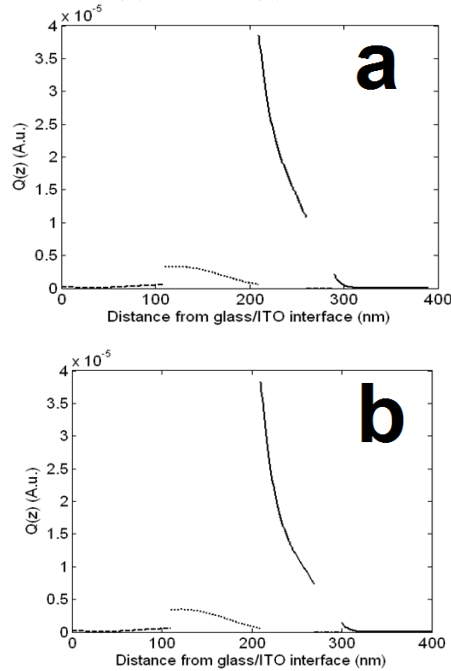


Fig. 11. Q Versus distance from SiO_2/ITO interface, (a): $d=50\text{nm}$; (b): $d=60\text{nm}$

In this structure, we consider $L_d=20\text{nm}$ that the maximum efficiency obtained. Also, the Diagram of η_{IQE} is depicted in Fig. 12.

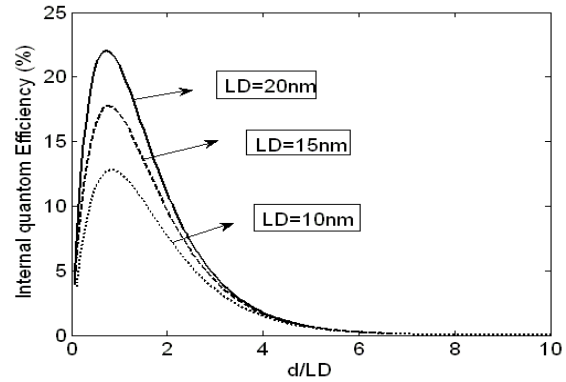


Fig. 12. Internal quantum efficiency versus d/L_D in various diffusion lengths for arrangement 2

In this optimal thickness, $\eta_{IQE}=5/8\%$ and $J_{sc}=1/33 \text{ mA/cm}^2$. In P_m point, $J_m=1.25 \text{ mA/cm}^2$, $V_m=0.15\text{v}$ and $FF=0.7$ are achieved. As a result, $PCE=2/86\%$.

With comparison of 2 structures, we conclude that with adding the PEDOT:PSS layer PCE increases to amount of 0.62% .

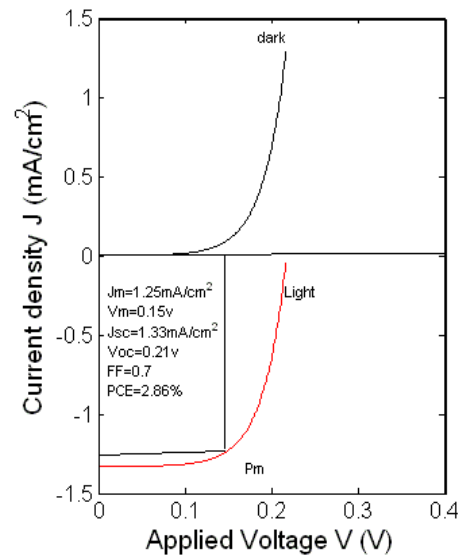


Fig. 13. Current density versus applied voltage under dark and light for arrangement 2

Table 1. Comparison of both proposed arrangements

| Arrangements | $J_{sc} \left(\frac{\text{mA}}{\text{cm}^2} \right)$ | $V_{oc} (\text{v})$ | $J_m \left(\frac{\text{mA}}{\text{cm}^2} \right)$ | $V_m (\text{V})$ | FF | PCE (%) |
|--|---|---------------------|--|------------------|------|---------|
| $\text{SiO}_2/\text{ITO}/\text{Cupc}/\text{C}_{60}/\text{Al}$ | 1.16 | 0.21 | 1 | 0.16 | 0.66 | 2.44 |
| $\text{SiO}_2/\text{ITO}/\text{pedot}/\text{Cupc}/\text{C}_{60}/\text{Al}$ | 1.33 | 0.21 | 1.25 | 0.14 | 0.7 | 2.86 |

4. Summary and conclusion

In summary, an optical simulation based on matrix model was carried out using of performance of a solar cell for exciton and photocurrent generation considering the maximum diffusion length for this structure.

Results show that with adding PEDOT:PSS layer between anode and CuPc, PCE increases to amount of 0.62% due to internal electric field increment that causes in turn the enhancement of the efficiency.

A comparative study on the results reveals that the optimal thickness with high absorption value in the case of blend layer can be determined. The results also show that, the optical and electrical parameters of the layers are completely correlated with each other. With these results, it would be possible to optimize the optical absorption processes in the solar cells and also propose structures with high efficiency.

References

- [1] C. J. Brabec, *Sol. Energy Mater. Sol. Cells*, **83**, 273 (2004).
- [2] P. Peumans, A. Yakimov, S. R. Forrest, *J. Appl. Phys.*, **93**, 3693 (2003).
- [3] L. Liu, G. Li, *Solar Energy Materials & Solar Cells* **95**, 2557 (2011).
- [4] Y. Kim, S. A. Choulis, J. Nelson, D. D. C. Bradley, S. Cook, J. R. Durrant, *Appl. Phys. Lett.* **86**, 063502 (2005).
- [5] V. Perraki, *Solar Energy Materials & Solar Cells* **94**, 1597 (2010).
- [6] R. A. Street, *Applied Physics Letters* **93**, 133308 (2008).
- [7] P. V. Kamat, *J. Phys. Chem. C*, **112**, 18737 (2008).
- [8] Xi Xi, Wenjia Li, Jiaqi Wu, Jingjia Ji, Zhengrong Shi, Guohua Li, *Solar Energy Materials & Solar Cells* **94**, 2435 (2010).
- [9] Nils-Krister Persson, Olle Inganas, *Solar Energy Materials & Solar Cells* **90**, 3491 (2006).
- [10] H. Y. Chen, J. H. Hou, S. Q. Zhang, Y. Y. Liang, G. W. Yang, Y. Yang, L. P. Yu, Y. Wu, G. Li, *Nat. Photonics* **3**, 649 (2009).
- [11] C. Lungenschmied, G. Dennler, H. Neugebauer, S. N. Sariciftci, M. Glatthaar, T. Meyer, A. Meyer, *Sol. Energy Mater. Sol. Cells* **91**, 379 (2007).
- [12] F. C. Krebs, *Sol. Energy Mater. Sol. Cells* **93**, 465 (2009).
- [13] Mikkel Jørgensen, Kion Norrman, Frederik C. Krebs, *Solar Energy Materials & Solar Cells* **92**, 686 (2008).
- [14] G. Yu, J. Gao, J. C. Hummelen, F. Wuld, A. J. Heeger, *Science* **270**, 1789 (1995).
- [15] Y. Y. Liang, Z. Xu, J. B. Xia, S. T. Tsai, Y. Wu, G. Li, C. Ray, L. P. Yu, *Adv. Mater.* **22** (2010).
- [16] M. Reyes-Reyes, K. Kim, D. L. Carroll, *Appl. Phys. Lett.* **87**, 083506- 1 (2005).
- [17] T. Soga, *Nanostructured material for solar energy conversion*, Elsevier (2007).
- [18] Sh. A. Furman, A. V. Tikhonravov, *Basics of Optics of Multilayer Systems*, Frontiers, Paris, 1996.
- [19] J. Lund, R. Roge, R. Peterson, Tom Larsen, *Polymer Solar Cells* (2006).
- [20] Nils-Krister Persson, Olle Inganas, Copyright 2005 by Taylor & Francis Group, LLC.
- [21] L. A. A. Pettersson, L. S. Roman, O. Inganas, *Journal of Applied Physics* **86**(1), 487 (1999).
- [22] H. Hoppe, N. Arnold, N. S. Sariciftci, D. Meissner, *Solar Energy Materials and Solar Cells* **80**(1), 105 (2003).
- [23] N.-K. Persson, M. Schubert, O. Inganas, *Solar Energy Materials and Solar Cells* **83**(2-3), 169 (2004).

*Corresponding author: azizian@uma.ac.ir,
yashar.a.k@gmail.com